Developmental Cell
Article

Genome-Wide RNAi Screens Identify Genes Required for Ricin and PE Intoxications

Dimitri Moreau,[1] Pankaj Kumar,[1] Shyi Chyi Wang,[1] Alexandre Chaumet,[1] Shin Yi Chew,[1] Hélène Chevalley,[1] and Frédéric Bard[1,*]
[1]Institute of Molecular and Cell Biology, 61 Biopolis Drive, Proteos, Singapore 138673, Singapore
*Correspondence: fbard@imcb.a-star.edu.sg
DOI 10.1016/j.devcel.2011.06.014

SUMMARY

Protein toxins such as Ricin and Pseudomonas exotoxin (PE) pose major public health challenges. Both toxins depend on host cell machinery for internalization, retrograde trafficking from endosomes to the ER, and translocation to cytosol. Although both toxins follow a similar intracellular route, it is unknown how much they rely on the same genes. Here we conducted two genome-wide RNAi screens identifying genes required for intoxication and demonstrating that requirements are strikingly different between PE and Ricin, with only 13% overlap. Yet factors required by both toxins are present from the endosomes to the ER, and, at the morphological level, the toxins colocalize in multiple structures. Interestingly, Ricin, but not PE, depends on Golgi complex integrity and colocalizes significantly with a medial Golgi marker. Our data are consistent with two intertwined pathways converging and diverging at multiple points and reveal the complexity of retrograde membrane trafficking in mammalian cells.

INTRODUCTION

Ricin is a plant protein with high toxicity present in high concentration in the beans of *Ricinus communis*. Because of its stability and relative ease of preparation, it represents a potential biological weapon. *Pseudomonas* exotoxin A (PE) is a protein secreted by *Pseudomonas aeruginosa*, an opportunistic pathogen that affects immunocompromised patients, causing pulmonary and urinary tract infections as well as infections of burn injuries (Wolf and Elsässer-Beile, 2009).

Although from different origins, both PE and Ricin share a similar mode of action: hijacking cellular processes to cross the cell membrane and targeting protein synthesis. Like many other toxins, PE and Ricin bind cell surface receptors that are endocytosed. After internalization, some toxins, such as diphtheria, are able to translocate from the endosomal lumen to the cytosol (Ratts et al., 2003). Ricin, PE, Shiga, and other toxins instead hijack retrograde membrane transport to traffic from the endosomes to the Golgi and from there to the ER (Sandvig et al., 2010).

In the lumen of the ER, these toxins are thought to interact with elements of the ER-associated degradation (ERAD) pathway, which targets misfolded proteins in the ER for degradation. This interaction is proposed to allow translocation to the cytosol without resulting in toxin degradation (Johannes and Römer, 2010).

Obviously, this complex set of membrane-trafficking and membrane-translocation events involves many host proteins, some of which have already been described (Johannes and Römer, 2010; Sandvig et al., 2010). Altering the function of these host proteins could in theory provide a toxin antidote.

Consistently, inhibition of retrograde traffic by drugs such as Brefeldin A (Sandvig et al., 1991) (Yoshida et al., 1991) or Golgicide A (Sáenz et al., 2009) and Retro-1 and 2 (Stechmann et al., 2010) can reduce intoxication of cultured cells by some toxins. In addition, Retro-2 can rescue mice challenged by Ricin nasal exposure (Stechmann et al., 2010). However, this drug may not be useful for other toxins because previous studies have revealed that different toxins can have different host gene requirements. For example, diphtheria toxin (DT) is highly dependent on clathrin, while Ricin can be internalized by independent mechanism(s) (Moya et al., 1985). Similarly, PE traffics between the Golgi and the ER in a COPI-dependent fashion by binding to KDEL receptor (KDELR), while Shiga toxin is COPI independent and Rab6 dependent (Wolf and Elsässer-Beile, 2009; Girod et al., 1999; White et al., 1999).

The molecular description of the retrograde-trafficking pathways remains limited with relatively few genes identified (Johannes and Popoff, 2008; Pavelka et al., 2008; Sandvig et al., 2010). As a consequence, it is not clear how much the requirements for host proteins of different toxins overlap. Interestingly, Ricin and PE, like diphtheria and Shiga toxins, all target the mammalian translation machinery (Hartley and Lord, 2004; Falnes and Sandvig, 2000).

This allowed us to use the same assay and very similar experimental conditions to reliably compare the gene sets required for different toxins. We present two genome-wide RNAi screens identifying human genes required for Ricin and PE intoxication. Our results reveal a large number of genes required for maximal toxic effect, some of them previously known to be involved in membrane traffic. Furthermore, we find that the requirements for both toxins differ significantly and at multiple levels. Interestingly, the toxins also share genetic requirements and similar subcellular localizations at various levels of their trafficking, suggesting two intertwined pathways converging and diverging at multiple levels.

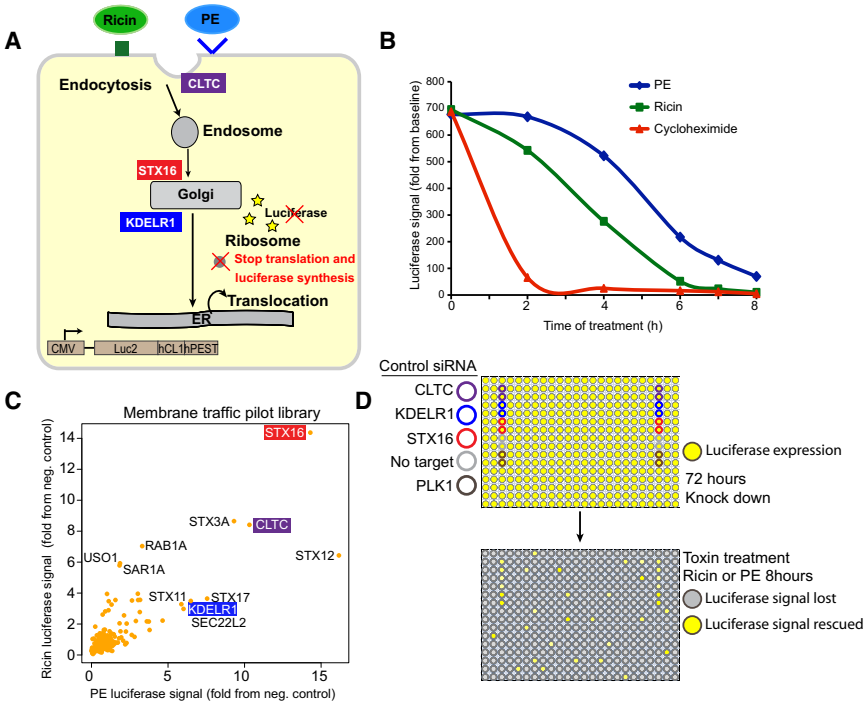

Figure 1. High-Throughput siRNA Screening of Retrograde Transport of PE and Ricin Toxin

(A) Intoxication assay using HeLa cells stably expressing a luciferase with short half-life (Luc2CP). After binding at the cell surface, both toxins are internalized into endosomes and transported to the Golgi and then the ER, where they translocate to the cytosol. Both toxins then inhibit translation and luciferase production. Luciferase activity rapidly drops because of the short half-life of the protein due to the hCL1 and hPEST destabilization sequences fused at the C-terminal end. The three highlighted genes, CLTC1, STX16, and KDELR1, act on endocytosis, transfer to the Golgi, and Golgi to ER traffic, respectively.

(B) Time course of luciferase signal from cells exposed to PE (0.25 ng/ml), Ricin (250 ng/ml), or cycloheximide (20 μg/ml).

(C) Membrane-traffic pilot library (201 genes) screens: luciferase values are expressed in fold from the negative control and plotted on x axis for PE treatment and y axis for Ricin treatment.

(D) Work flow of the genome-wide screen (run in duplicate): cells are seeded in 384-well plates preprinted with siRNA for reverse transfection and incubated for 72 hr, then challenged with Ricin or PE for 8 hr before luciferase signals are measured.

RESULTS

A Pilot Screen Identifies STX16 as an Important Regulator of Both Ricin and PE Traffic

Ricin and PE intoxicate cells by inhibiting protein synthesis. To measure this effect, we used a destabilized luciferase with a short half-life as previously described (Zhao and Haslam, 2005) (Figure 1A). In this assay, cells challenged by 25 ng/ml PE or 250 ng/ml Ricin almost completely lose their luciferase signal after about 8 hr (Figure 1B), which was therefore used as the endpoint for the screens.

Knockdown of a gene important for intoxication will rescue the luciferase signal in toxin-treated cells. To identify positive controls to use for screen quality control and data normalization, we performed a pilot screen on a library of siRNA pools targeting 201 known membrane-trafficking regulators (Figure 1C). This library was designed to target all identified human SNARES, which are essential regulators of membrane traffic, and previously described regulators of toxin trafficking such as KDELR1, Rab6a, and the clathrin heavy chain (CLTC). Knockdown of most SNARES did not significantly rescue intoxication by either toxins; however, loss of Syntaxins 3, 12, and 16 provided some of the strongest rescue observed (Figure 1C).

Interestingly, whereas it was reported that Syntaxin 16 (STX16) is important for endosome to trans-Golgi network (TGN) retrograde traffic (Amessou et al., 2007; Pérez-Victoria and Bonifacino, 2009; Ganley et al., 2008), Syntaxins 3 and 12 have not been previously associated with retrograde traffic. Syntaxin 12 has been linked to endosomal membrane fusion (Prekeris et al., 1998; McBride et al., 1999), so it could be involved in the sorting of toxins at the endosome level. Syntaxin 3, on the other hand, is thought to mediate fusion events at the plasma membrane (Low et al., 2006); therefore, its likely role in regard to toxin trafficking is less obvious.

Because STX16 showed a strong inhibition of both PE and Ricin trafficking, we chose it as one of our positive controls in the screen (Figure 1D). We also selected CLTC, which affected both toxins but more significantly PE. This is consistent with previous reports where PE has been shown to be dependent on clathrin-mediated endocytosis, whereas Ricin also uses clathrin-independent mechanisms (Moya et al., 1985; Sandvig et al., 1987). Finally, we also selected KDELR1 because its knockdown provides a modest inhibitory effect specifically for PE intoxication.

Whole-Genome Screens for PE and Ricin Reveal a Large Number of Potent Regulators of Toxin Trafficking

Whole-genome screens were performed in duplicate using the library siGENOME SMARTpool siRNAs that targets 21,121 human genes with one pool of four siRNAs per gene. Following reverse transfection, cells were incubated for 72 hr and then challenged with PE or Ricin for 8 hr before luminescence reading (Figure 1C).

Reproducibility between duplicates was high for both screens with average Spearman rank correlations between the replicates of 0.85 for PE and 0.84 for Ricin (see Figure S1 available online). For normalization, we realized that the usual plate-based z-score normalization method was inadequate because of the non-random organization of the library. For example, some strong regulators of the assay, members of the proteasome complex, are clustered in the library. This is apparent in the variations of z-score for the STX16 controls that are more pronounced than variations in raw values (Figures 2A and 2B). Given the stability in the raw values of the controls, we decided to normalize the

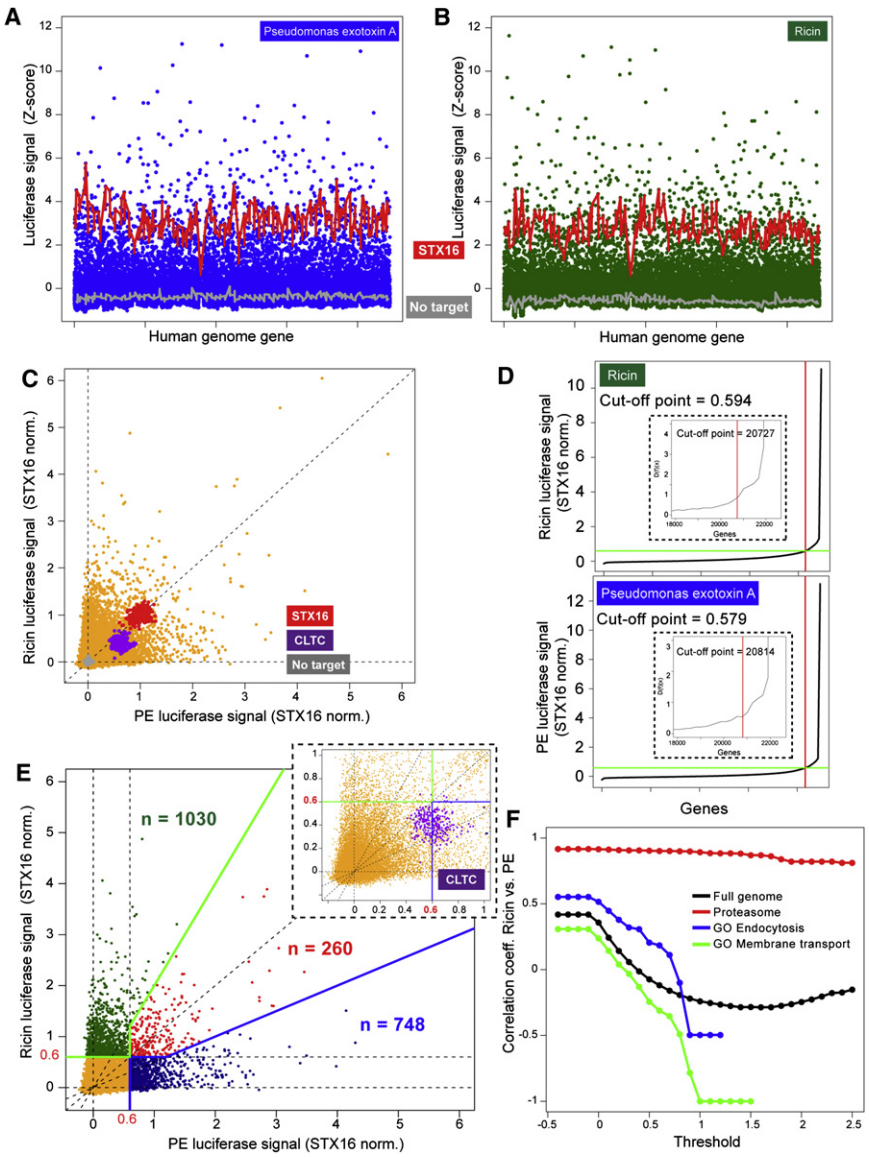

Figure 2. Genome-Wide Screen Analysis Reveals Significant Differences between PE and Ricin Host Genetic Requirements

(A and B) Luciferase signal z-scores for ~22,000 human genes; PE values represented in blue (A) and Ricin in green (B). Gray and red lines correspond to negative control (nontarget siRNA) and positive control (STX16 siRNA), respectively.

(C) STX16-normalized luciferase signals for Ricin versus PE screens. Red, purple, and gray dots correspond, respectively, to STX16, CLTC, and nontarget control wells.

(D) Determination of significance threshold values using derivative method. Ranked data (main plots) and their derivative (inset) are used to determine a significance threshold. For both toxins the threshold was set at 0.6 (60% of STX16 average inhibition). This threshold defines 2038 genes whose knockdown triggers significant inhibition.

(E) Same plot as (C) with significance and specificity threshold lines: blue for Ricin and green for PE. Blue, red, and green dots correspond to Ricin-specific, common, and PE-specific hits, respectively. Inset shows a zoom in with the distribution of CLTC control values in the screen in relation to threshold values.

(F) Correlation coefficient between Ricin and PE data as a function of STX16-normalized threshold levels shows that both toxins have very different requirements. Black, all genes; green, genes with a GO related to membrane transport; blue, genes with a GO related to endocytosis process; red, genes related to the proteasome (highly correlated because they affect directly luciferase levels).

For both (C) and (D), the figure can be zoomed in to reveal gene names inside the nodes. (See also Figure S1.)

data to the average per plate of anti-STX16 siRNA and nontarget siRNA wells (formula in Experimental Procedures). Using this normalization, the values of controls had a more compact distribution, and therefore this method should provide a more accurate normalization (Figure 2C).

Surprisingly, analysis of the raw data revealed numerous genes with a stronger inhibition of intoxication than our strongest control STX16 (Figures 2A–2C). To define a functionally significant threshold, we used the first derivative of the ranked data set to detect the point at which we can observe a steep rise. This indicated that signals equal or greater that 60% of STX16 inhibition are significantly above genomic noise (Figure 2D and Experimental Procedures). This threshold also corresponds with the average PE value for the CTLC positive control (inset, Figure 2E). For comparison, it corresponds in most assay plates to a z-score of about 2. Using this threshold, we identified 2038 factors as potential regulators of either toxin trafficking.

To define toxin specificity, we next considered that a strong inhibition of a specific membrane-traffic pathway could affect indirectly and to a lesser extent a different pathway. Therefore, a fixed threshold value for toxin specificity (dotted lines in Figure 2E) could be misleading. Instead, we used a 2-fold difference of inhibition between the two toxins as an indicator of specificity and derived corresponding cutoff values (diagonal green and blue lines in Figure 2E; see also Experimental Procedures). Within these thresholds, the number of genes that affect both toxins similarly is surprisingly small (260), representing about 13% of the total. The two toxin-specific groups are much larger, with 1030 and 748 genes affecting Ricin and PE intoxication, respectively. Consistently, the two screens show a low correlation coefficient that drops quickly below zero as the significance threshold increases (Figure 2F). By comparison, genes encoding for proteasome subunits show a strong correlation coefficient, which reflects their direct effect on the assay (see below). The low correlation between toxins is likely to reflect different requirements for retrograde membrane traffic of each toxin. Consistently, values for genes with biological process gene ontologies (GOs) related to endocytosis or membrane transport are in fact inversely correlated (Figure 2F).

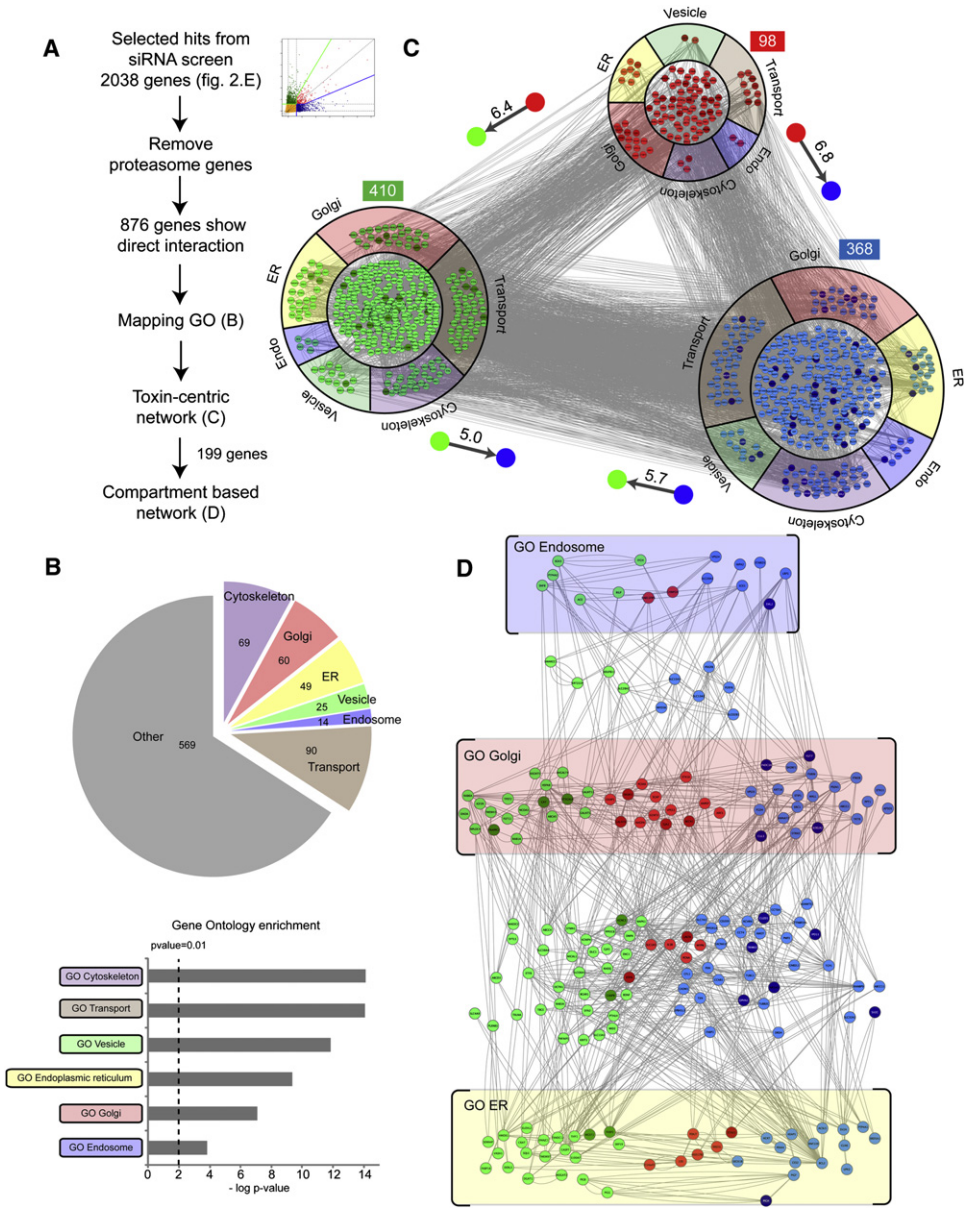

Figure 3. Protein Network Analysis of Hits Reveals a Highly Connected Common Set

(A) Procedure to determine the global direct interaction network between the 2038 hits identified in Figure 2E, followed by the generation of a network based on the subcellular location of hits.

(B) GO enrichment analysis on the directly connected hits, calculated using Fisher's exact test, shows statistically relevant ($p < 0.01$) enrichments of genes involved in membrane traffic.

(C) Global direct interaction network between all connected hits from each category (Ricin-specific, green; PE-specific, blue; common, red). Each category is classified into membrane traffic-related subcategories identified by GO analysis. Arrows and numbers represent the average number of connections from one group to another.

(D) Network based on genes with ontology related to a cellular compartment involved in the transport of Ricin and PE traffic and the first level interactors of these genes. (See also Figure S2.)

Network Analysis Reveals a Shared Machinery for Intoxication

Analysis of the GO of the 2038 genes within our thresholds revealed that almost 50% of those having GO were related to membrane compartments or membrane-transport processes (Figure S2). These results are consistent with the known biology of these toxins, which are thought to rely on host genes mostly for transport from the cell surface to the cytosol.

We next analyzed how these various genes may interact with each other. The 2038 genes were screened to remove proteasome-related genes, and the STRING protein-protein interactions database was searched with the remainder (Figure 3A).

A total of 876 were found to have a direct link to another hit in the screen (Figure 3A). Among these, 35% (307) had either a cellular component GO related to membrane compartments or a biological process GO related to membrane transport, these types of GOs being significantly enriched in this data set (Figure 3B). We then subdivided the 876 factors into three groups depending on their toxin specificity (Figure 3C).

Next, we analyzed the connectivity between each of the three groups. Because the number of nodes (or genes) is different among the three groups, we chose to compare groups by dividing the total number of edges (connections) between a source group and a target group by the number of nodes in the target group. Interestingly, the factors required for both toxins (subsequently referred to as common genes or factors; red nodes in Figure 3) form on average 6.8 connections with the Ricin group (green nodes), whereas the PE group (blue nodes) shares only 5.7 edges with the Ricin group. Similarly, common genes have on average 6.9 connections with the PE group versus 5.0 from Ricin to PE group (Figure 3C). This striking difference in connectivity suggests that common factors are more likely to be hubs in the cell protein-protein network.

The nodes of the network (genes) were also organized within each group based on cellular component GO information (Figure 3C). This approach revealed that toxin-specific factors are not enriched within any specific compartment (endosomes, Golgi, or ER), suggesting that trafficking of the two toxins differs at multiple levels. At the same time, the common genes are also equally represented in these various compartments, suggesting that both toxins also share requirements at various levels of toxin traffic. To further organize the network based on known subcellular localization of the factors, we selected genes with a cellular component GO linked to endosomes, Golgi, or ER and their direct interactors. This procedure isolated a subset of 202 genes (Figure 3D) that provides a preliminary map of the retrograde traffic process. This map was used to extract further insights into complexes required for intoxication by either PE or Ricin (see Figures 5 and 6).

Limited Overlap with Yeast Requirements for K28 Toxin Traffic but Good Reproducibility in MG63 Human Cells

A recent report isolated genes required for trafficking of the toxin K28 in yeast (Carroll et al., 2009). K28 is a protein toxin that follows COPI-dependent retrograde trafficking and inhibits protein synthesis in yeast cells. Given that both mammalian-specific toxins have significantly different host gene requirements, we wanted to assess how yeast toxin requirements compare with the two mammalian toxins we tested.

The 165 genes identified to be required in yeast were mapped into the NCBI HomoloGene database, generating 144 distinct homolog IDs, which had 50 corresponding human genes (Figure S3A). These 50 human genes were in turn mapped onto our screen results (Figure S3B). Of the 50 genes, 8 had a significant effect on intoxication by either Ricin or PE. Interestingly, whereas three of them have been linked to toxins and/or membrane-trafficking processes, the other five are associated with unrelated processes. The relatively limited overlap between yeast and mammalian requirements for A-B toxins probably reflects in part the imprecision in mapping genes between distant genomes but also reinforces the notion that multiple retrograde pathways probably exist.

We next evaluated whether the genetic information obtained in our screens was valid in a different human cell line. MG63, an osteosarcoma cell line, was selected because it expresses high levels of PE receptor and was used for this reason to study the subcellular distribution of PE (see below) (Niemeier et al., 2005). MG63 cells were transiently transfected with siRNAs corresponding to selected hits (Figure 4D and Table S3) and the destabilized luciferase construct (Figure S3C). We then compared the rescue obtained in MG63 and in HeLa cells and found a good overall correlation (Figure S3D), indicating that our data are not cell line dependent.

178 Regulators of Ricin or PE Intoxication Confirmed by at Least Two Independent siRNAs

To confirm the results of the primary screen for a subset of genes highly likely to be directly involved in retrograde membrane traffic, the first 200 hits in both screens were identified using RSA ranking method, which takes into account both signal intensity and reproducibility (Figure 4A) (König et al., 2007). Because both PE and Ricin have been shown to induce some programmed cell death, we excluded genes involved in apoptosis using GO. The luciferase assay by itself is evidently highly sensitive to perturbations of luciferase expression and of the protein degradation machinery; therefore, we next excluded all genes with a GO related to these processes (Figure 4A).

The remaining 235 genes were tested for their ability to affect luciferase signal upon treatment with cycloheximide to detect genes with toxin-independent effects. As expected, the proteasomal gene PSMD2 responded strongly in this assay (Figure 4B), and seven other genes were eliminated. The significant effect of Sec61B in this assay was a surprise because the translocon has not been reported to control general protein degradation and because Sec61B showed a strong bias for PE (see Figure 6D), which is not expected for a regulator of protein degradation. This inconsistency was later resolved (see below).

To select genes for which an off-target effect is highly unlikely, we tested individually each of the four siRNAs that constitute the pools used in the primary screen. We found, as previously reported, that individual siRNAs tend to be less potent than the pools (Parsons et al., 2009). Therefore, we defined validated individual siRNAs using a threshold signal of 30% that of STX16 pool, and validated genes as those having at least two validated individual siRNAs (Figure 4C). Using these criteria, 178 genes were identified as regulators of toxin retrograde traffic (Figure 4D and Table S1) with about 24% (44) affecting both toxins and a roughly equal number (65 and 69) affecting each toxin specifically (Figure 4D).

Shiga Intoxication Assay Reveals a Limited Overlap with Ricin Requirements

We next tested how these 178 genes could affect intoxication with Shiga, a commonly studied toxin with similar trafficking and protein inhibition properties (Sandvig et al., 2010). Because STX16 has an inhibitory effect on Shiga intoxication similar to its effect on Ricin and PE (data not shown), we used the same 60% STX16 significance threshold and identified 44 genes that affect this toxin (Figure 4E). A larger proportion (~40%) of the common

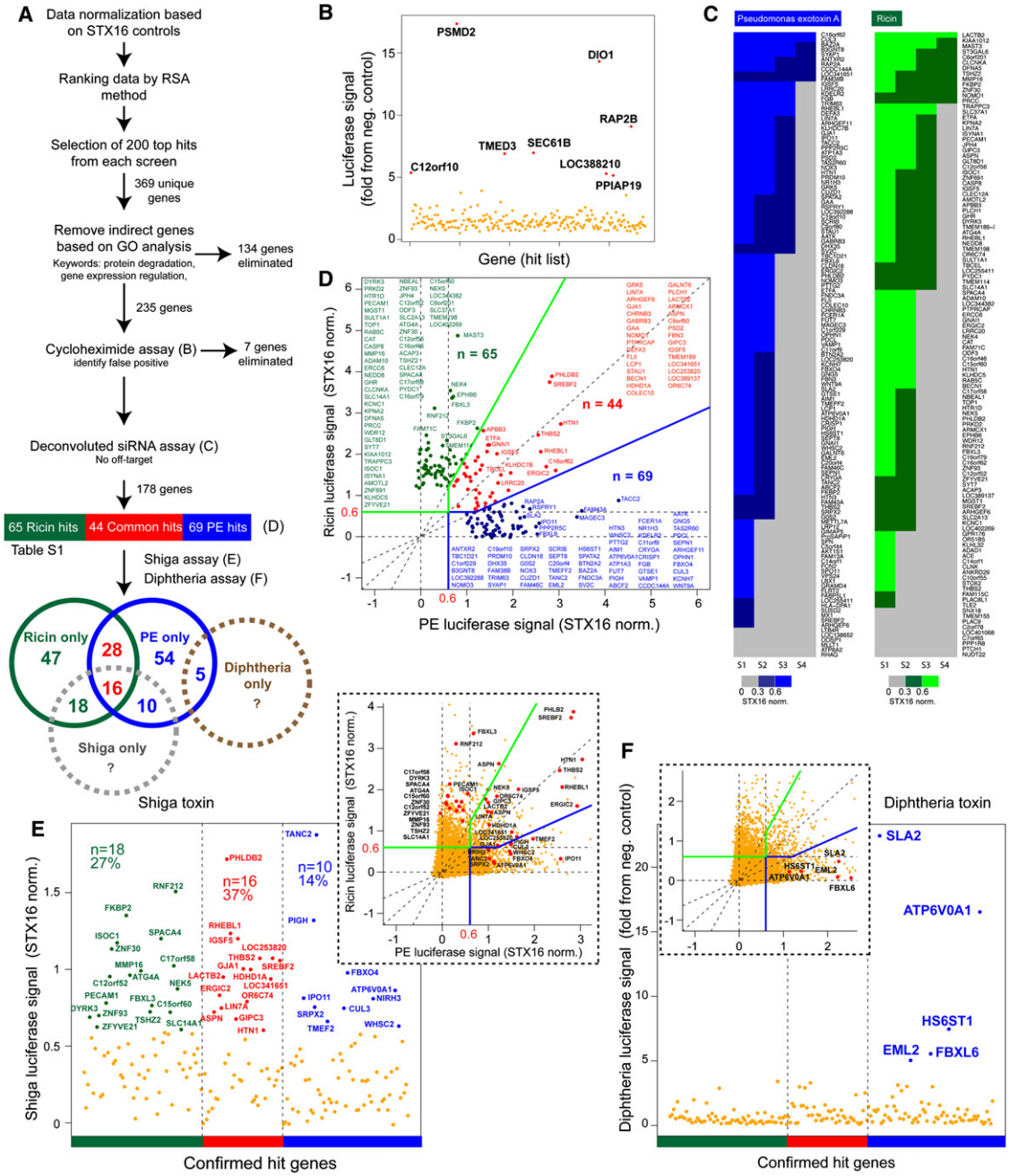

Figure 4. Validation Assays and Comparison with Two Other A/B Toxins, Shiga Toxin and DT

(A) Flow chart for the validation procedure. The 200 top hits were selected in each screen using a ranking-based method (RSA), and the resulting 369 unique genes were manually curated using GO database to remove genes unlikely to be directly related to toxin transport.

(B) Identification of genes able to rescue luciferase signal after cycloheximide treatment. These genes are false positive (proteasome gene PSMD2 is an expected false positive). Using a cutoff of inhibition five times higher than negative control, seven genes were identified and excluded (red-labeled dots).

(C) Exclusion of off-target RNAi effects using deconvoluted siRNA pools. Luciferase assay was run with 4 individual duplex siRNAs for each of the 228 genes. Each set of four duplexes is ranked based on rescue efficacy. A gene is validated if at least two unique siRNAs gave a STX16-normalized value higher than 0.3.

(D) Plot of validated hits, color coded as in Figure 2E.

(E) Shiga intoxication assay on the validated genes. The data are normalized to STX16 average values. A total of 44 genes show a value above a 0.6 cutoff. Percentages indicate the amount of Ricin, PE, or common hits that show also an effect for Shiga toxin. Inset shows the values of those genes in the two genome-wide screens.

(F) Diphtheria intoxication assay on the validated genes. Results are expressed as fold of the negative control. Five genes show a value above the 5-fold chosen as significance threshold. Inset shows the value of those genes in the two genome-wide screens. (See also Figure S3.)

pool is essential for Shiga intoxication, suggesting that they could be required for multiple toxins besides the three we tested. Shiga toxin appears to share only a limited pool of specific factors with Ricin (27%) and even less with PE (14%) (Figure 4E). The results of this assay are compiled in Table S3.

Five Confirmed Genes Also Block Diphtheria Intoxication

Similarly to PE, DT catalyzes the transfer of an ADP-ribosyl onto elongation factor 2, resulting in a block in protein synthesis (Zhang et al., 2010). However, DT does not traffic to the ER but instead translocates to the cytosol at the endosome level (Johannes and Decaudin, 2005).

As therefore expected, we found that diphtheria intoxication is not sensitive to STX16 knockdown. Among the 178 genes that were confirmed to be important for either PE or Ricin intoxication (Figure 4F), only five (SLA2, ATP6V0A1, EML2, FBXL6, and HS6ST1) inhibited diphtheria intoxication at least 5-fold over the negative control upon knockdown (Figure 4F). This low number is consistent with the shorter intracellular route of diphtheria. All five factors were required specifically for PE and not Ricin, suggesting that diphtheria and PE subvert similar endosomal physiology (Figure 4F, inset).

Interestingly, whereas Ricin is able to be endocytosed by clathrin-independent mechanisms, PE and diphtheria have been reported to depend on clathrin for their endocytosis (Garred et al., 2001; Moya et al., 1985). Consistent with diphtheria's intracellular trafficking, three of the five factors identified can be linked to endocytosis or endosome physiology. SLA2, which provides a strong protective effect against both PE and diphtheria (Figure 4F and inset), has been implicated in downregulation of growth factor receptors (Pandey et al., 2002). The proton pump-encoding gene ATP6V0A1 is required for endosome acidification, which is required for both diphtheria and PE toxins for their insertion in membranes (Ratts et al., 2003; Méré et al., 2005). EML2 is homologous to the sea urchin microtubule-associated protein EMAP and is associated with microtubules in mitotic human cells (Eichenmuller et al., 2002). However, it has also been reportedly found on intracellular membrane-bound organelles in interphase cells that are reminiscent of endosomes (Barbe et al., 2008). Microtubules are known to be important for endosomal maturation (Driskell et al., 2007), suggesting that EML2 may mediate endosome traffic on microtubules.

Known Regulators of Membrane Trafficking Are Identified in the Screens

Our screen results are consistent with published research on toxin trafficking because we identified at least 17 genes previously implicated in toxin trafficking (Table S2). Some negative results are due to the toxicity of the siRNA used against some genes (Table S2). Others, such as for the genes encoding the COG complex, were probably due to inefficient knockdown because we found in later experiments that COG gene knockdown significantly blocks Ricin intoxication (data not shown).

One of the surprises of the screens was the relatively low number of bona fide membrane-trafficking players present among the most potent inhibitors of intoxication upon knockdown. However, analysis of the 2038 potential regulators revealed numerous genes clearly linked to membrane traffic (Table S3). These included several SNARES, small GTPases of the Rab family and Rab-interacting proteins, Arf3, and various factors such as the BARS protein. Consistent with the results of our GO analysis, most of these factors were specific for one toxin.

By contrast, five factors implicated in the control of sterol synthesis are required for both toxins, with a sixth, NR1H3, falling close to our specificity threshold (Figure S3E). This is consistent with the known requirement of cholesterol for the retrograde traffic of multiple toxins (Grimmer et al., 2000; Oda and Wu, 1994; Lippincott-Schwartz and Phair, 2010). It also illustrates the consistency of the screen results in relation to toxin specificity.

Similarly, two members of the GARP complex, VPS53 and VPS54, have similar effects on both intoxications, although VPS54 falls just below our cutoff values (Figure 5A). The third member of the complex, VPS52, is likely to be a false negative (Figure 5B). The GARP complex is proposed to mediate docking of transport carriers at the TGN and was recently shown to interact with STX16 (Pérez-Victoria and Bonifacino, 2009). Our results suggest that GARP and STX16 mediate docking and fusion of both Ricin- and PE-containing transport carriers (Figures 5A and 5B).

Interestingly, the v-SNARE reported by Pérez-Victoria and Bonifacino (2009) to interact with GARP, VAMP4, rescues specifically Ricin intoxication, albeit slightly below our significance threshold (52% of STX16 rescue for Ricin and 5% for PE). This suggests that Ricin and PE traffic from endosomes to Golgi in different carriers with different associated v-SNAREs.

Consistent with this notion, VPS35, a central component of the Retromer, a complex proposed to function in the formation of transport carriers at the endosomes and destined for the Golgi (Johannes and Popoff, 2008), rescues only PE and not Ricin (Figures 5A and 5B). Of note, several proteins that have been shown in complex with the Retromer but not implicated in membrane traffic, including XPO7, SFN, and ARHGAP1 (Mingot et al., 2004), display similar rescue effects as the sorting nexin SNX1, a bona fide member of the Retromer (Bonifacino and Hurley, 2008).

The three subunits TRAPPC2, 3, and 8 all strongly rescue Ricin but not PE intoxication (Figures 5A and 5B), displaying highly correlated specificity. The TRAPP complex is known to be essential for Golgi integrity, and we could confirm a strong perturbation of Golgi marker distributions in our experimental conditions (data not shown) (Yu et al., 2006). Similarly, knockdown of genes of the COG complex blocked significantly only Ricin intoxication (data not shown). These results indicate that PE trafficking surprisingly does not require the integrity of the Golgi apparatus.

ERGIC 2 Is an Important Regulator of Golgi-to-ER Traffic

ERGIC2 is among the relatively few genes related to membrane trafficking whose knockdown provides a strong rescue for Ricin, PE, and Shiga toxins (Figures 4D, 4E, and 5A). Knockdown with three independent siRNAs confirmed the on-target effect (data not shown). Independent repeats showed a very significant 65%–85% rescue of luciferase signal from nontreated cells 8 hr after exposure to the toxins (Figure 5C).

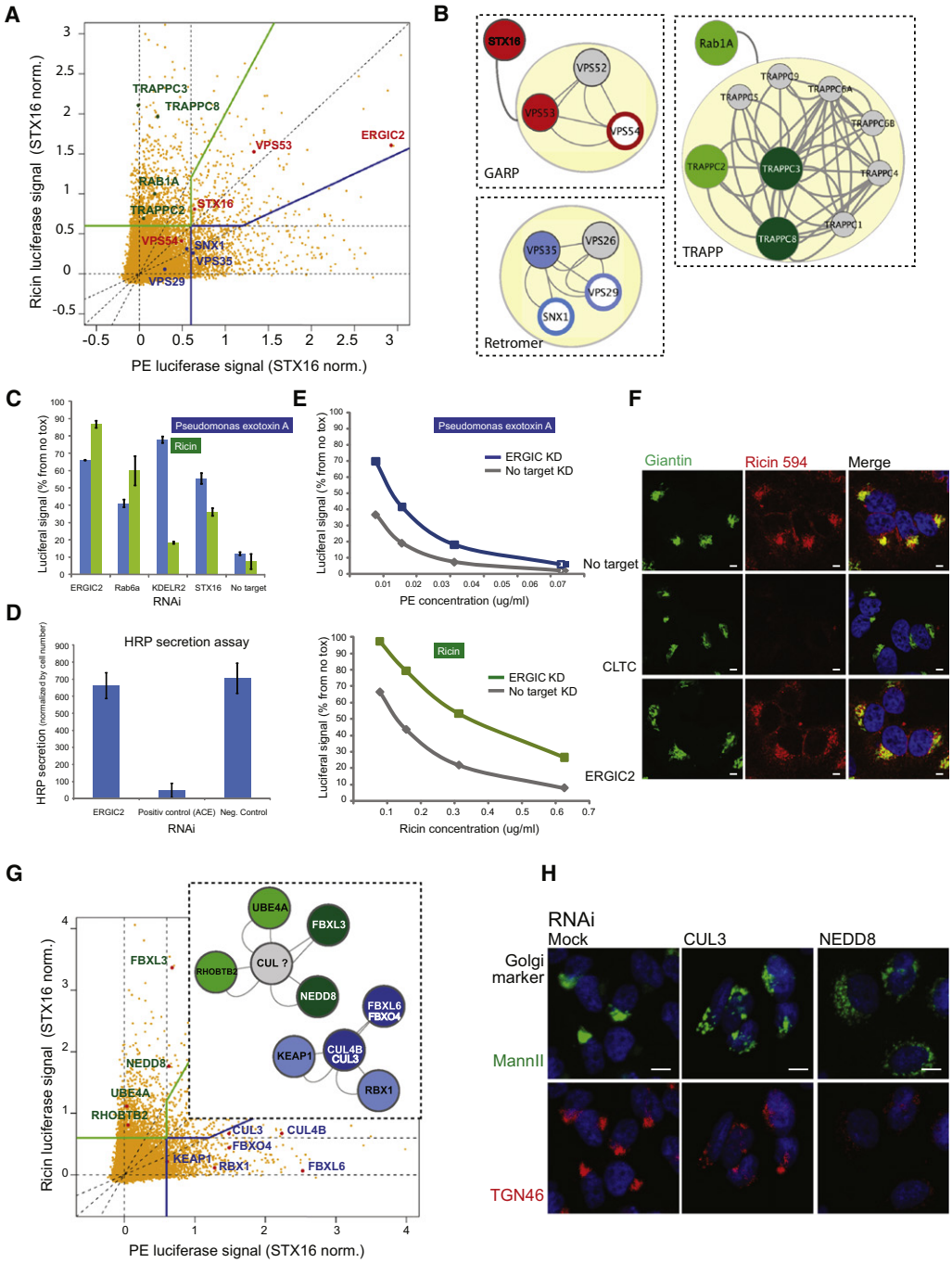

Figure 5. Noticeable Protein Complexes and Pathways Involved in Ricin and PE Trafficking

(A) 2D plots are based on values of STX16-normalized luciferase signals in primary Ricin and PE screens. Specific factors shown in (B) and for ERGIC2 are highlighted.

(B) Three known protein complexes, GARP, Retromer, and TRAPP, with interacting partners are shown with interactions found in STRING. Color code for nodes: green is Ricin-specific hit, blue is PE-specific hit, red is common hit, gray is nonhit, darker color with white letters for validated hit, and colored circle for genes below but close to threshold. Large yellow discs delineate known protein complexes from interacting factors.

(C) Comparison of the rescue level of ERGIC2 with known factors regulating Golgi to ER traffic and STX16 expressed as a percentage of luciferase signal in cells not exposed to any toxin.

(D) Secreted HRP activity (luminescence normalized to cell number) upon ERGIC2 knockdown, compared to positive (ACE gene) and negative controls. Error bars represent SEM for both (C) and (D).

(E) Dose-response curves to Ricin and PE toxins in conditions of ERGIC2 knockdown.

(F) Intracellular localization of Ricin labeled with Alexa 594 internalized by HeLa cells for 40 min. Comparison of cell knockdown for the Clathrin gene CTLC and ERGIC2.

By contrast, knockdown of ERGIC2 did not result in any significant inhibition of general secretion, as measured by exogenously expressed secreted HRP (Figure 5D) (Bard et al., 2006). These data suggest that ERGIC2 could represent an interesting therapeutic target to develop a toxin antidote. Consistent with this proposal, ERGIC knockdown shows rescue even at relatively high doses of toxin, especially for Ricin (Figure 5F). ERGIC2 is a homolog of the yeast protein Erv41p, which has been shown to cycle between ER and Golgi and interact with Erv46 (Otte et al., 2001), suggesting that it could mediate trafficking of the toxins between the Golgi and the ER. Consistent with this idea, ERGIC2 knockdown showed accumulation of fluorescently labeled Ricin at the Golgi, as defined by Giantin staining (Figure 5).

Different Cullin-RING Ligases Are Required for Ricin and PE Intoxication

Among the complexes identified using network information, some of the surprises are the Cullin-Ring Ligases (CRLs). CRLs are multisubunit ubiquitin ligases that regulate various aspects of cell and organism physiology (Petroski and Deshaies, 2005). Multiple related genes for each member of the typical complex have been described.

Among PE hits, four out of five members of the usual complex are present (SKP1 being the exception) (Figure 5G) (Petroski and Deshaies, 2005). The presence of two Cullins (CUL3 and CUL4B) and two F-box proteins (FBXO4 and FBXL6) suggests the existence of two functionally independent complexes regulating PE intoxication and possibly sharing the ring protein RBX1 and the substrate adaptor KEAP1.

Interestingly, among the Ricin hits, different members of the same type of complex are present, including the F-box protein FBXL6, UBEA4, the substrate adaptor RHOBTB2, and the neddylation factor NEDD8 (Figure 5G). The clear specificity of NEDD8 for Ricin is surprising because neddylation has been proposed to regulate most types of CRLs (Skaar and Pagano, 2009) (Figure 5G).

The CRLs have been implicated in numerous biological processes but not, until recently, in membrane traffic (Petroski and Deshaies, 2005). Marino Zerial's laboratory reported recently that some CRLs appear to be involved in endosome maturation (Collinet et al., 2010). Consistently, the effect of FBXL6 knockdown on diphtheria intoxication suggests that the related complex may function at the endosome level (Figure 4E). To test if some of these genes could regulate the endosomal to Golgi retrograde traffic of an endogenous protein, TGN46, knockdown was performed in cells expressing the Golgi marker MannII-GFP, which were then stained for TGN46. Strikingly, NEDD8 knockdown resulted in a strong reduction of TGN46 signal at the Golgi, and both NEDD8 and CUL3 knockdown induced extensive Golgi fragmentation (Figure 5H).

A Common ER Lumen Set of Chaperones for Ricin and PE

Upon reaching the ER, toxins such as Ricin and PE have been proposed to engage the ERAD pathway (Johannes and Popoff, 2008). ERAD is a process by which misfolded proteins in the ER are extruded to the cytosol for degradation by the proteasome (Vembar and Brodsky, 2008).

Consistent with this proposal, knockdowns of the ER lumen chaperones PDILT or ERO1L are able to strongly rescue both PE and Ricin intoxication (Figure 6E). ERO1L or ERO1A can oxidize protein disulfide isomerases such as PDILT, and both types of proteins are associated with the ERAD pathway (Brodsky and Wojcikiewicz, 2009). ER chaperones are known to also mediate the oxidoreduction of cysteine bridges in endogenous proteins and toxins, probably explaining the importance of the FAD-dependent oxidoreductase domain-containing protein FOXRED2. Two other chaperones of the ER lumen, FKBP2 and PDI4A, are specific, respectively, for Ricin and PE (Figure 6E).

Ricin and PE Use Different ER Membrane Translocation Channels

Engagement of the ERAD pathway by toxins is thought to result ultimately in the toxin's translocation to the cytosol (Johannes and Römer, 2010). Two main types of translocation channels have been described so far: the Sec61 translocon and the complex formed by Derlins.

Knockdown of Sec61B in the primary screen resulted in a strong rescue of PE intoxication. However, Sec61B knockdown also rescued the luciferase signal after cycloheximide treatment (Figure 4B), suggesting an indirect effect. To sort out these contradictory results, each subunit of the translocon (A1, A2, B, and G) was tested with four independent siRNAs (Figure 6A). The cycloheximide rescue assay demonstrated that a single siRNA (marked with red star in Figure 6A) against Sec61B had a strong and probably off-target effect. Yet, the involvement of the translocon in PE translocation was nevertheless confirmed by the other siRNAs. Consistently, a mix of the single most potent siRNAs against A1, A2, G, and B (excluding the off-targeting suspect) resulted in a strong and specific rescue of PE but not Ricin intoxication (Figure 6B).

Ricin, by contrast, appears to rely on Derlins: DERL3 was found positive and confirmed in the main screen, and individual siRNAs against DERL1 and 2 showed significant and specific effects (Figure 6A). Similarly, a mix of siRNAs against the three Derlins resulted in significant rescue of Ricin but not PE intoxication (Figure 6B). Because only a single siRNA validated both Derlin 2 and 3, we repeated knockdown with a set of siRNA pools from a different supplier and were able to confirm the specific role of the Translocon and the Derlin complexes in PE and Ricin intoxications, respectively (Figure 6C).

The specific role of Derlins for Ricin translocation across ER membranes is consistent with the additional identification of UFD1L and NPLOC4 as Ricin-specific factors (Figure 6E). Indeed, these two factors form with the ATPase VCP a ternary complex that is required for protein export from the ER and has been shown to bind to Derlins (Oda et al., 2006).

Interestingly, the Shiga toxin relies on the Translocon and not the Derlins (Figure 6C). To verify that knockdown of translocon genes does not affect the cell surface presentation of a protein

(G) Same as (A) for genes related to CRL complexes. Inset shows the interactions in the potential CRL complexes involved as found in STRING. No Cullin specific for Ricin was identified.
(H) Effect of CUL3 and NEDD8 knockdown on the distribution of two different Golgi markers, Mannosidase II and TGN46 (scale bars are 10 μm).

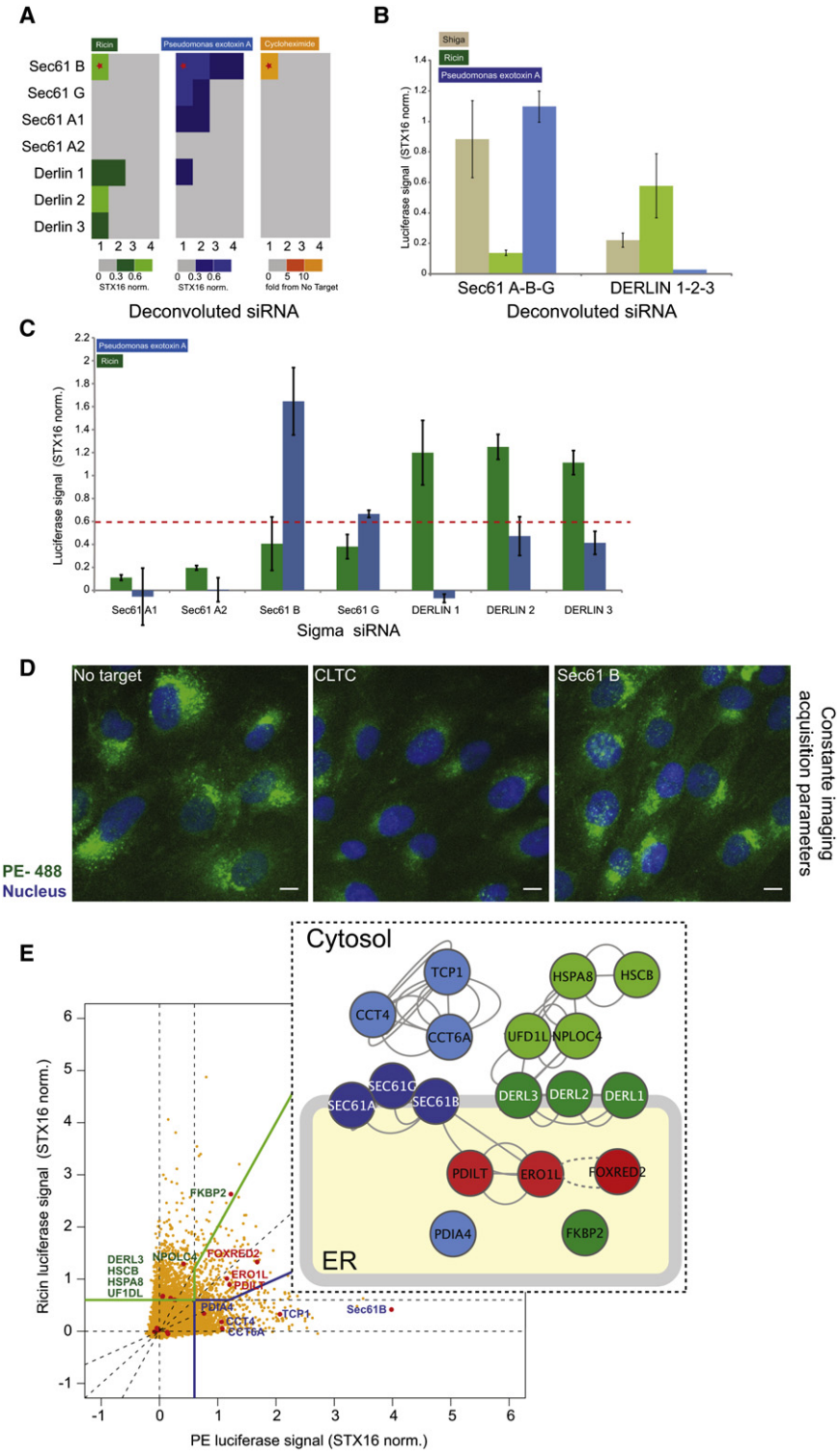

Figure 6. Toxin Interaction with the ERAD Pathway and Cytosolic Chaperonins

(A) Individual siRNAs from the pools used in primary screen tested for rescue of luciferase signal after Ricin, PE, and cycloheximide exposure. Signals are STX16 normalized and color coded according to threshold values. Red star denotes a single siRNA against Sec61B with potential off-target effect.

(B) STX16-normalized luciferase signals for Ricin (green), Shiga (beige), or PE (blue) after knockdown using siRNA pools comprising the best individual siRNA for each gene of the Sec61 complex or the Derlins.

(C) Confirmation screen with siRNA pools different from the primary screen against genes of the Sec61 translocon and the three Derlins. Error bars represent SEM for both (B) and (C).

(D) Internalization of PE labeled with Alexa 488 in MG63 cell knockdown for CLTC gene and Sec61B gene.

(E) 2D plot of STX16-normalized luciferase signals in primary screens for Ricin and PE rescue with ERAD-related genes highlighted. Inset is a schematic of subcellular localization of the labeled genes. In the ER lumen, both toxins require PDILT and ERO1L. Color codes for nodes are identical to Figure 5.

required for PE binding and internalization such as LRP1, the intracellular amount of PE labeled with Alexa 488 was evaluated by fluorescence microscopy (Figure 6D). Our positive control CTLC showed significant reduction of internalized PE-A488, whereas Sec61B knockdown resulted in normal accumulation of PE in the perinuclear area.

Potential Cytosolic Refolding Factors for Toxins

Interaction with the ERAD machinery and translocation through the ER membranes implies the unfolding of the toxins. However, to exert their toxic effects in the cytosol, the toxins need to avoid degradation and refold. Toxins are thought to escape degradation by virtue of the low number of lysines that they contain (Johannes and Popoff, 2008). However, so far, little is known about the mechanisms mediating toxin refolding.

Three members of the TCP1 ring complex, CCT4, CCT6A, and TCP1 itself, are found specifically required for PE intoxication (Figure 6E). This complex is known to assist the folding of various proteins such as actin and tubulin (Burns and Surridge, 1994) and may therefore promote the refolding of PE after its translocation. Several other cytosolic chaperones specific for PE are also identified but cannot be connected to other factors.

In the Ricin-specific group, HSPA8 and HSCB are two heat-shocked cognate proteins of the HSP70 family known to mediate protein folding (Figure 6E). Interestingly, the UFD1L, NPLOC1, and VCP complex has been shown to interact with HSP70 family proteins, suggesting that they may function in sequence during Ricin translocation and refolding.

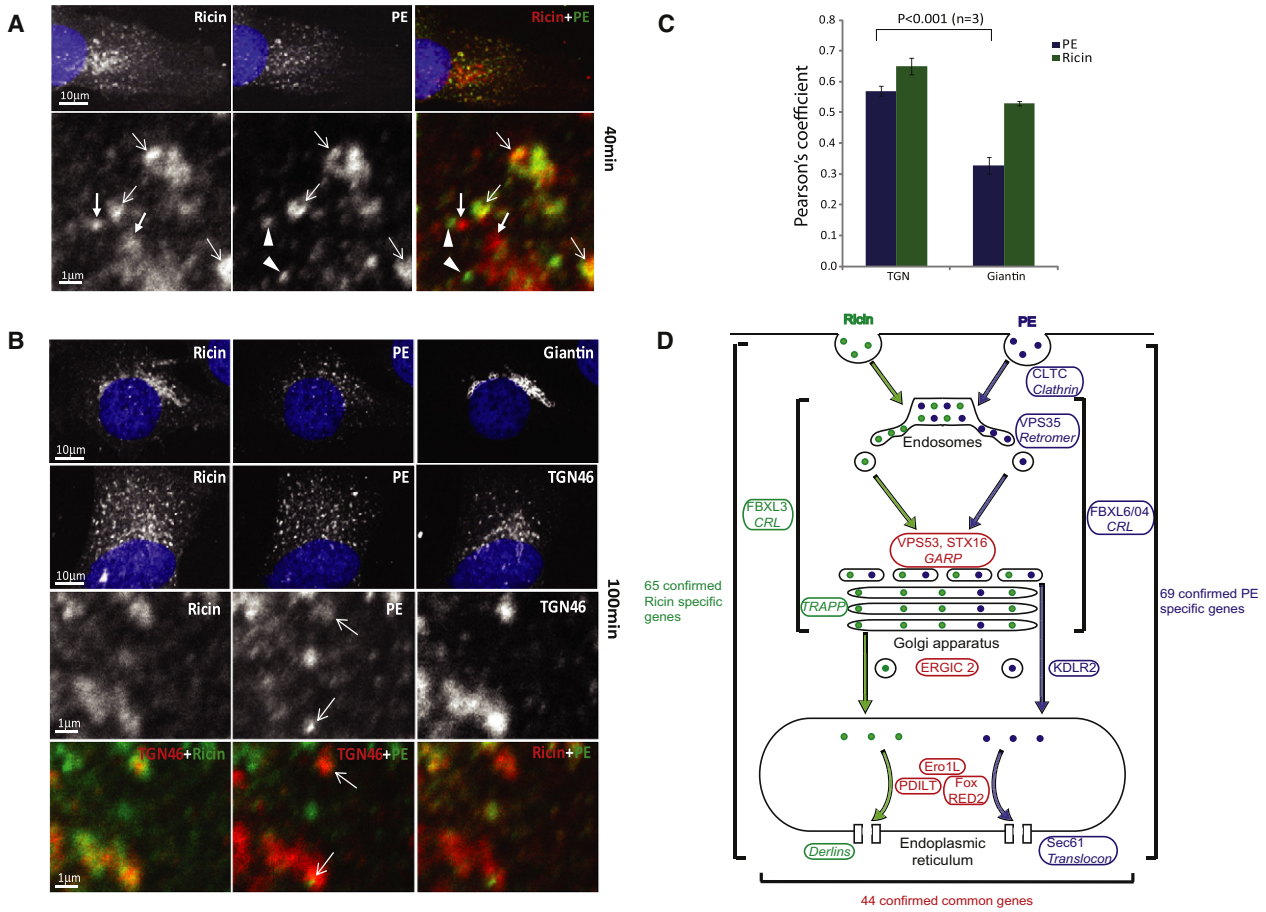

Figure 7. PE and Ricin Intracellular Distributions

(A–C) MG-63 cells were exposed to both PE labeled with Alexa 488 and Ricin labeled with Alexa 594 and fixed 40 or 100 min after toxin exposure.

(A) Thick arrows point to Ricin-specific structures, arrowheads to PE-specific structures, and thin arrows to structures with colocalization of both toxins.

(B) At later time points, Ricin colocalizes extensively with Giantin-labeled Golgi structures, whereas PE only colocalizes with some TGN-labeled structures (thin arrows).

(C) Fluorescence Pearson's correlation coefficients between each toxin and the two Golgi markers were calculated using ImageJ JACoP plug-in. Student's t test shows a statistically significant difference between the correlations of PE/TGN and PE/Giantin. Error bar represents SEM.

(D) Hypothetical model depicting how PE and Ricin travel from extracellular space to the ER with some identified genes highlighted.

Differences in Intracellular Trafficking of Fluorescently Labeled Ricin and PE

The marked differences in genetic requirements between PE and Ricin suggest that the two toxins rely on different membrane-bound transport carriers. To test this, HeLa cells were exposed to PE labeled with Alexa 488 and Ricin labeled with Alexa 594. Unfortunately, HeLa cells tend to internalize only small amounts of PE, making any visualization arduous. MG63 cells by contrast express generously the PE receptor LRP1 and were therefore used for visualization experiments (Niemeier et al., 2005). At early time points after internalization, we found that PE and Ricin colocalize in large vesicular structures (Figure 7A). In addition, multiple small vesicular structures appeared to be enriched in either one or the other toxin, suggesting toxin-specific sorting events. At later time points after internalization, Ricin appeared to accumulate readily in the Golgi cisternae as labeled by Giantin (Figure 7B). By contrast, PE, although it accumulates in the perinuclear area, could be detected in the Golgi only in much lower amounts. Interestingly, PE appeared to colocalize better with the TGN marker TGN46 than Giantin (Figure 7B). Quantification of the Pearson's correlation coefficient between PE and TGN46 or Giantin fluorescence signals confirmed this trend (Figure 7C), suggesting that PE is able to reach the TGN compartment but not the medial Golgi. By contrast, Ricin appears able to access equally the TGN and the medial Golgi (Figures 7B and 7C).

DISCUSSION

Our screens have revealed that Ricin and PE rely on different membrane-trafficking pathways at multiple stages. Consistently, fluorescently labeled toxins can be found in different vesicular structures. However, they also colocalize in large endocytic structures, suggesting convergence after internalization into a common compartment. This might be why, at the genetic level, both toxins depend on a common set of endosome-related

genes such as the ESCRT component VPS2 (CHMP2A), Rab11FIP, and Rab5c. From this endocytic compartment, the toxins appear to be sorted again into different carriers en route to the Golgi, with PE specifically depending on the Retromer. The endosomal-derived carriers probably converge at the TGN with colocalization of the two toxins with the TGN46 marker and a common requirement on the GARP complex and the SNARE STX16.

Interestingly, the toxins appear to diverge again at this stage. Ricin becomes enriched in the *cis*- and medial-Golgi compartments, and its toxicity is dependent on the Golgi-related complexes TRAPP (Figure 5A) and COG (data not shown). By contrast, PE is found in lower amounts in the medial Golgi and is insensitive to knockdown of genes from either Golgi complexes, suggesting a bypass of the core Golgi complex. Interestingly, the KDELR, which binds and is required by PE, has been shown to retrieve peptides with C-terminal KDEL directly from the TGN (Miesenböck and Rothman, 1995).

Overall, our data suggest that several similar and intertwined retrograde membrane-trafficking pathways coexist (Figure 7D). The reason for such intricacy remains unclear, but it could provide the means for the differential regulation of trafficking of endogenous factors. Membrane-trafficking events underlie the formation and maintenance of membrane-bound cell compartments. The number and specialization of these compartments have increased with evolution, augmenting the complexity of cellular compartmentalization. Examples of this increase include but are not limited to the Golgi apparatus itself, the various secretory granules found in specialized cells, and the plasma membrane domains in epithelial cells and in neurons. The genetic complexity we uncovered probably reflects the perhaps underappreciated complexity of compartmentalization in nondifferentiated human cells.

Our study also provides a number of potential therapeutic targets to design specific toxin antidotes. Understanding and targeting specific pathways will likely allow a better control of possible side effects. The high number of genes involved also suggests that synergistic drug therapies against this type of toxins could be designed.

EXPERIMENTAL PROCEDURES

Chemical Reagents

The genome-wide siRNA library human siGENOME was obtained from Dharmacon (now Thermo-Fisher). Luciferase was detected with One-Glo (Promega). Ricin was obtained from Sigma, PE and DT from Merck, and Shiga toxin from Toxin Technology.

Cell Cultures and Cloning

All plasmids were cloned using Gateway technology (Invitrogen). For the luciferase reporter the luc2CP sequence was isolated from pGL4.16 (Promega) by PCR and cloned in pLenti-6.3 (Invitrogen). Lentiviruses were generated following the instruction of the manufacturer (Invitrogen). Wild-type (WT) HeLa cells were transduced by lentivirus to stably express Luc2CP or KDELR-GFP. All cell lines are grown in Dulbecco's modified Eagle's medium (DMEM), high glucose, supplemented with 10% fetal calf serum, at 37°C in a 10% CO_2 incubator. ERGIC1, 2, and 3 cDNAs were cloned from HeLa WT mRNA in the pcDNA40, including an N-terminal GFP tag. Luminal domain mutants were generated by PCR mutagenesis removing amino acids 47–244 for ERGIC1, 55–307 for ERGIC2, and 49–336 for ERGIC3.

Screen Assay

All knockdown experiments were performed in 384-well plates (384 black μclear; Greiner), and all liquid dispensing was performed using a Multidrop Combi (Thermo Fisher Scientific). Reverse transfection was performed at 25 nM siRNA with 7.25 μl Opti-MEM (GIBCO, Invitrogen) and 0.25 μl HiPerFect (QIAGEN) per well. After 20 min complex formation, 2500 (for Ricin screen) or 5000 (for PE screen) HeLa Luc2CP cells were added to each well. After 72 hr, the medium was removed, and cells were treated with 25 μl of toxin for final concentrations of 250 ng/ml Ricin or 0.25 ng/ml PE. After 8 hr, luciferase activity was revealed with One-Glo and the luminescence signal acquired using an Infinite M200 luminometer (Tecan). Similar conditions were used for DT at 6 ng/ml (Merck), Shiga toxin at 200 ng/ml (Toxin Technology), and cycloheximide at 20 μg/ml (Invitrogen).

Data Formatting and Normalization

Genome-wide RNAi screening data, luciferase signal intensities were normalized plate by plate based on samples or on controls (Birmingham et al., 2009). In sample-based normalization, z-score was calculated using the following formula: $Z = (x_i - \overline{x})/\sigma_x$, where x_i is luciferase signal intensity of the gene i, $\overline{x}$ is average of the of luciferase signal intensities of all the genes per plate, and σ_x is the standard deviation of luciferase signal intensities of the genes per plate. Control (STX16)-normalized score was calculated using the following formula: $(STX16)Normalized\ Score = x_i - \overline{x}_p/\overline{x}_p - \overline{x}_n$, where x_i is the luciferase signal intensity of the gene i, $\overline{x}_p$ is average of the luciferase signal intensity values of positive controls (STX16) per plate, and $\overline{x}_n$ is average of the luciferase signal values of negative controls (GFP) per plate.

Cutoff Determination for Selecting Primary Hits

For each PE and Ricin screen, first derivative method was employed to find the ranked gene after which there is sharp increase in STX16-normalized score. The first derivative was calculated using the following formula: $D(f)(x) = f(x+\Delta) - f(x-\Delta)/2\Delta$, where $f(x)$ represents the STX16-normalized score of gene of rank x. Genes are ranked in ascending order of their STX16-normalized scores. Δ is the minimal incremental interval (1 in this case). This gene number where $D(f)(x)$ showed a steep rise was selected as cutoff value (20,727 for Ricin and 20,814 for PE) with a corresponding STX16-normalized score of 0.594 for Ricin and 0.579 for PE. Therefore, 0.6 was chosen as cutoff value for both toxins. Toxin specificity boundaries were generated using the following conditions:

PE-specific region = ((PE STX16 normalized > 2 × threshold) AND (Ricin STX16 normalized < ½ PE STX16 normalized)) ∪ ((PE STX16 normalized > threshold) AND (Ricin STX16 normalized < threshold) AND (PE STX16 normalized < 2 × threshold)).

Ricin-specific region = ((Ricin STX16 normalized > 2 × threshold) AND (Ricin STX16 normalized > 2 × PE STX16 normalized)) ∪ ((Ricin STX16 normalized > threshold) AND (PE STX16 normalized < threshold) AND (Ricin STX16 normalized < 2 × threshold)).

Common region = (PE STX16 normalized > threshold) AND (Ricin STX16 normalized > threshold) AND (Ricin STX16 normalized < ½ PE STX16 normalized) AND (Ricin STX16 normalized > 2 × PE STX16 normalized).

Correlation between PE and Ricin

Correlation coefficient (r) of all the genes above threshold was calculated between STX16-normalized score of PE and Ricin using the following formula:

$$r = \frac{\sum_{i=1}^{n}(x_i - \overline{x})(y_i - \overline{y})}{\sqrt{\sum_{i=1}^{n}(x_i - \overline{x})^2}\sqrt{\sum_{i=1}^{n}(y_i - \overline{y})^2}},$$

where x_i is STX16-normalized score of gene i in Ricin screen above the threshold, $\overline{x}$ is average of the of STX16-normalized scores of the all the genes above threshold in Ricin Screen, y_i is STX16-normalized score of gene i in PE screen above the threshold, $\overline{y}$ is average of the of STX16-normalized scores of the all the genes above threshold in PE screen, and n is the total number of genes above threshold. The gene set and total number of genes above threshold change based on the specific GO criteria: full genome (all genes), proteasome-related genes, and endocytosis or membrane transport-related

genes. The plot of correlation coefficient was generated for different thresholds starting from −0.5 to 2.5 with the interval of 0.1.

Protein Networks

The protein network was created by STRING (Jensen et al., 2009) and imported in Cytoscape (Killcoyne et al., 2009; Shannon et al., 2003) for further annotation of gene attributes using GO (Ashburner et al., 2000) and NCBI Gene database, network analysis, and custom visualization. Network nodes were further classified as PE specific, Ricin specific, and common nodes based on the predefined boundaries. Genes in the network were categorized based on different GO terms associated, and the enrichment for these categories was calculated using Fisher's exact test (Huang et al., 2009).

Screen Quality Control

The control of RNAi screening data quality for both PE and Ricin toxin was done using cellHTS2 (Boutros et al., 2006). The two replicates were evaluated by Spearman rank correlation coefficient, a nonparametric test. The average Spearman rank correlations between the replicates are 0.85 for PE and 0.84 for Ricin (maximum value is 1). The Z′ scores of both screens were 0.27 for PE and 0.24 for Ricin, which is quite normal for RNAi screening (Birmingham et al., 2009).

Fluorescent Toxin Internalization

PE and Ricin were labeled according to manufacturer's instructions (Invitrogen). MG-63 cells were seeded 1 day before toxin binding. Cells were pretreated with hypotonic medium (DMEM culture diluted 1:1 with water) for 20 min at 37°C and incubated with an estimated 200 μg/ml of fluorescent toxins for an additional 40 or 100 min. Cells were washed with PBS before being fixed with 4% paraformaldehyde and 4% sucrose in PBS for 30 min.

Imaging and Image Analysis

Confocal images were acquired using Olympus FluoView Confocal Microscope (model IX81; Olympus) with a 100× objective (UPLSAPO; NA 1.40). Wide-field images were acquired using Molecular Device ImageXpress Micro automated fluorescent microscope with a 40× objective. Image analysis was done using granularity module from MetaXpress, and the data were processed with AcuityXpress.

SUPPLEMENTAL INFORMATION

Supplemental Information includes three figures and four tables and can be found with this article online at doi:10.1016/j.devcel.2011.06.014.

ACKNOWLEDGMENTS

We thank the Experimental Therapeutic Centre of Singapore for its help with screening operations, the Harvard Medical School Screening Facility for kindly allowing us to use the ScreenSaver software, and the IMCB COM-IT for developing a screening-related software. This work was funded by the Institute of Molecular and Cell Biology and the Agency for Science, Technology and Research (A*STAR) of Singapore.

Received: October 7, 2010
Revised: February 21, 2011
Accepted: June 9, 2011
Published online: July 21, 2011

REFERENCES

Amessou, M., Fradagrada, A., Falguières, T., Lord, J.M., Smith, D.C., Roberts, L.M., Lamaze, C., and Johannes, L. (2007). Syntaxin 16 and syntaxin 5 are required for efficient retrograde transport of several exogenous and endogenous cargo proteins. J. Cell Sci. *120*, 1457–1468.

Ashburner, M., Ball, C.A., Blake, J.A., Botstein, D., Butler, H., Cherry, J.M., Davis, A.P., Dolinski, K., Dwight, S.S., Eppig, J.T., et al; The Gene Ontology Consortium. (2000). Gene ontology: tool for the unification of biology. Nat. Genet. *25*, 25–29.

Barbe, L., Lundberg, E., Oksvold, P., Stenius, A., Lewin, E., Björling, E., Asplund, A., Pontén, F., Brismar, H., Uhlén, M., and Andersson-Svahn, H. (2008). Toward a confocal subcellular atlas of the human proteome. Mol. Cell. Proteomics *7*, 499–508.

Bard, F., Casano, L., Mallabiabarrena, A., Wallace, E., Saito, K., Kitayama, H., Guizzunti, G., Hu, Y., Wendler, F., Dasgupta, R., et al. (2006). Functional genomics reveals genes involved in protein secretion and Golgi organization. Nature *439*, 604–607.

Birmingham, A., Selfors, L.M., Forster, T., Wrobel, D., Kennedy, C.J., Shanks, E., Santoyo-Lopez, J., Dunican, D.J., Long, A., Kelleher, D., et al. (2009). Statistical methods for analysis of high-throughput RNA interference screens. Nat. Methods *6*, 569–575.

Bonifacino, J.S., and Hurley, J.H. (2008). Retromer. Curr. Opin. Cell Biol. *20*, 427–436.

Boutros, M., Brás, L.P., and Huber, W. (2006). Analysis of cell-based RNAi screens. Genome Biol. *7*, R66.

Brodsky, J.L., and Wojcikiewicz, R.J.H. (2009). Substrate-specific mediators of ER associated degradation (ERAD). Curr. Opin. Cell Biol. *21*, 516–521.

Burns, R.G., and Surridge, C.D. (1994). Functional role of a consensus peptide which is common to alpha-, beta-, and gamma-tubulin, to actin and centractin, to phytochrome A, and to the TCP1 alpha chaperonin protein. FEBS Lett. *347*, 105–111.

Carroll, S.Y., Stirling, P.C., Stimpson, H.E.M., Giesselmann, E., Schmitt, M.J., and Drubin, D.G. (2009). A yeast killer toxin screen provides insights into a/b toxin entry, trafficking, and killing mechanisms. Dev. Cell *17*, 552–560.

Collinet, C., Stöter, M., Bradshaw, C.R., Samusik, N., Rink, J.C., Kenski, D., Habermann, B., Buchholz, F., Henschel, R., Mueller, M.S., et al. (2010). Systems survey of endocytosis by multiparametric image analysis. Nature *464*, 243–249.

Driskell, O.J., Mironov, A., Allan, V.J., and Woodman, P.G. (2007). Dynein is required for receptor sorting and the morphogenesis of early endosomes. Nat. Cell Biol. *9*, 113–120.

Eichenmuller, B., Everley, P., Palange, J., Lepley, D., and Suprenant, K.A. (2002). The human EMAP-like protein-70 (ELP70) is a microtubule destabilizer that localizes to the mitotic apparatus. J. Biol. Chem. *277*, 1301–1309.

Falnes, P.O., and Sandvig, K. (2000). Penetration of protein toxins into cells. Curr. Opin. Cell Biol. *12*, 407–413.

Ganley, I.G., Espinosa, E., and Pfeffer, S.R. (2008). A syntaxin 10-SNARE complex distinguishes two distinct transport routes from endosomes to the trans-Golgi in human cells. J. Cell Biol. *180*, 159–172.

Garred, Ø., Rodal, S.K., van Deurs, B., and Sandvig, K. (2001). Reconstitution of clathrin-independent endocytosis at the apical domain of permeabilized MDCK II cells: requirement for a Rho-family GTPase. Traffic *2*, 26–36.

Girod, A., Storrie, B., Simpson, J.C., Johannes, L., Goud, B., Roberts, L.M., Lord, J.M., Nilsson, T., and Pepperkok, R. (1999). Evidence for a COP-I-independent transport route from the Golgi complex to the endoplasmic reticulum. Nat. Cell Biol. *1*, 423–430.

Grimmer, S., Iversen, T.G., van Deurs, B., and Sandvig, K. (2000). Endosome to Golgi transport of ricin is regulated by cholesterol. Mol. Biol. Cell *11*, 4205–4216.

Hartley, M.R., and Lord, J.M. (2004). Cytotoxic ribosome-inactivating lectins from plants. Biochim. Biophys. Acta *1701*, 1–14.

Huang, W., Sherman, B.T., and Lempicki, R.A. (2009). Systematic and integrative analysis of large gene lists using DAVID bioinformatics resources. Nat. Protoc. *4*, 44–57.

Jensen, L.J., Kuhn, M., Stark, M., Chaffron, S., Creevey, C., Muller, J., Doerks, T., Julien, P., Roth, A., Simonovic, M., et al. (2009). STRING 8—a global view on proteins and their functional interactions in 630 organisms. Nucleic Acids Res. *37* (Database issue), D412–D416.

Johannes, L., and Decaudin, D. (2005). Protein toxins: intracellular trafficking for targeted therapy. Gene Ther. *12*, 1360–1368.

Johannes, L., and Popoff, V. (2008). Tracing the retrograde route in protein trafficking. Cell *135*, 1175–1187.

Johannes, L., and Römer, W. (2010). Shiga toxins—from cell biology to biomedical applications. Nat. Rev. Microbiol. *8*, 105–116.

Killcoyne, S., Carter, G.W., Smith, J., and Boyle, J. (2009). Cytoscape: a community-based framework for network modeling. Methods Mol. Biol. *563*, 219–239.

König, R., Chiang, C.-Y., Tu, B.P., Yan, S.F., DeJesus, P.D., Romero, A., Bergauer, T., Orth, A., Krueger, U., Zhou, Y., and Chanda, S.K. (2007). A probability-based approach for the analysis of large-scale RNAi screens. Nat. Methods *4*, 847–849.

Lippincott-Schwartz, J., and Phair, R.D. (2010). Lipids and cholesterol as regulators of traffic in the endomembrane system. Annu. Rev. Biophys. *39*, 559–578.

Low, S.H., Vasanji, A., Nanduri, J., He, M., Sharma, N., Koo, M., Drazba, J., and Weimbs, T. (2006). Syntaxins 3 and 4 are concentrated in separate clusters on the plasma membrane before the establishment of cell polarity. Mol. Biol. Cell *17*, 977–989.

McBride, H.M., Rybin, V., Murphy, C., Giner, A., Teasdale, R., and Zerial, M. (1999). Oligomeric complexes link Rab5 effectors with NSF and drive membrane fusion via interactions between EEA1 and syntaxin 13. Cell *98*, 377–386.

Méré, J., Morlon-Guyot, J., Bonhoure, A., Chiche, L., and Beaumelle, B. (2005). Acid-triggered membrane insertion of Pseudomonas exotoxin A involves an original mechanism based on pH-regulated tryptophan exposure. J. Biol. Chem. *280*, 21194–21201.

Miesenböck, G., and Rothman, J.E. (1995). The capacity to retrieve escaped ER proteins extends to the trans-most cisterna of the Golgi stack. J. Cell Biol. *129*, 309–319.

Mingot, J.-M., Bohnsack, M.T., Jäkle, U., and Görlich, D. (2004). Exportin 7 defines a novel general nuclear export pathway. EMBO J. *23*, 3227–3236.

Moya, M., Dautry-Varsat, A., Goud, B., Louvard, D., and Boquet, P. (1985). Inhibition of coated pit formation in Hep2 cells blocks the cytotoxicity of diphtheria toxin but not that of ricin toxin. J. Cell Biol. *101*, 548–559.

Niemeier, A., Kassem, M., Toedter, K., Wendt, D., Ruether, W., Beisiegel, U., and Heeren, J. (2005). Expression of LRP1 by human osteoblasts: a mechanism for the delivery of lipoproteins and vitamin K1 to bone. J. Bone Miner. Res. *20*, 283–293.

Oda, T., and Wu, H.C. (1994). Effect of lovastatin on the cytotoxicity of ricin, modeccin, Pseudomonas toxin, and diphtheria toxin in brefeldin A-sensitive and -resistant cell lines. Exp. Cell Res. *212*, 329–337.

Oda, Y., Okada, T., Yoshida, H., Kaufman, R.J., Nagata, K., and Mori, K. (2006). Derlin-2 and Derlin-3 are regulated by the mammalian unfolded protein response and are required for ER-associated degradation. J. Cell Biol. *172*, 383–393.

Otte, S., Belden, W.J., Heidtman, M., Liu, J., Jensen, O.N., and Barlowe, C. (2001). Erv41p and Erv46p: new components of COPII vesicles involved in transport between the ER and Golgi complex. J. Cell Biol. *152*, 503–518.

Pandey, A., Ibarrola, N., Kratchmarova, I., Fernandez, M.M., Constantinescu, S.N., Ohara, O., Sawasdikosol, S., Lodish, H.F., and Mann, M. (2002). A novel Src homology 2 domain-containing molecule, Src-like adapter protein-2 (SLAP-2), which negatively regulates T cell receptor signaling. J. Biol. Chem. *277*, 19131–19138.

Parsons, B.D., Schindler, A., Evans, D.H., and Foley, E. (2009). A direct phenotypic comparison of siRNA pools and multiple individual duplexes in a functional assay. PLoS ONE *4*, e8471.

Pavelka, M., Neumüller, J., and Ellinger, A. (2008). Retrograde traffic in the biosynthetic-secretory route. Histochem. Cell Biol. *129*, 277–288.

Pérez-Victoria, F.J., and Bonifacino, J.S. (2009). Dual roles of the mammalian GARP complex in tethering and SNARE complex assembly at the trans-golgi network. Mol. Cell. Biol. *29*, 5251–5263.

Petroski, M.D., and Deshaies, R.J. (2005). Function and regulation of cullin-RING ubiquitin ligases. Nat. Rev. Mol. Cell Biol. *6*, 9–20.

Prekeris, R., Klumperman, J., Chen, Y.A., and Scheller, R.H. (1998). Syntaxin 13 mediates cycling of plasma membrane proteins via tubulovesicular recycling endosomes. J. Cell Biol. *143*, 957–971.

Ratts, R., Zeng, H., Berg, E.A., Blue, C., McComb, M.E., Costello, C.E., vanderSpek, J.C., and Murphy, J.R. (2003). The cytosolic entry of diphtheria toxin catalytic domain requires a host cell cytosolic translocation factor complex. J. Cell Biol. *160*, 1139–1150.

Sáenz, J.B., Sun, W.J., Chang, J.W., Li, J., Bursulaya, B., Gray, N.S., and Haslam, D.B. (2009). Golgicide A reveals essential roles for GBF1 in Golgi assembly and function. Nat. Chem. Biol. *5*, 157–165.

Sandvig, K., Olsnes, S., Petersen, O.W., and van Deurs, B. (1987). Acidification of the cytosol inhibits endocytosis from coated pits. J. Cell Biol. *105*, 679–689.

Sandvig, K., Prydz, K., Hansen, S.H., and van Deurs, B. (1991). Ricin transport in brefeldin A-treated cells: correlation between Golgi structure and toxic effect. J. Cell Biol. *115*, 971–981.

Sandvig, K., Torgersen, M.L., Engedal, N., Skotland, T., and Iversen, T.G. (2010). Protein toxins from plants and bacteria: probes for intracellular transport and tools in medicine. FEBS Lett. *584*, 2626–2634.

Shannon, P., Markiel, A., Ozier, O., Baliga, N.S., Wang, J.T., Ramage, D., Amin, N., Schwikowski, B., and Ideker, T. (2003). Cytoscape: a software environment for integrated models of biomolecular interaction networks. Genome Res. *13*, 2498–2504.

Skaar, J.R., and Pagano, M. (2009). Control of cell growth by the SCF and APC/C ubiquitin ligases. Curr. Opin. Cell Biol. *21*, 816–824.

Stechmann, B., Bai, S.-K., Gobbo, E., Lopez, R., Merer, G., Pinchard, S., Panigai, L., Tenza, D., Raposo, G., Beaumelle, B., et al. (2010). Inhibition of retrograde transport protects mice from lethal ricin challenge. Cell *141*, 231–242.

Vembar, S.S., and Brodsky, J.L. (2008). One step at a time: endoplasmic reticulum-associated degradation. Nat. Rev. Mol. Cell Biol. *9*, 944–957.

White, J., Johannes, L., Mallard, F., Girod, A., Grill, S., Reinsch, S., Keller, P., Tzschaschel, B., Echard, A., Goud, B., and Stelzer, E.H. (1999). Rab6 coordinates a novel Golgi to ER retrograde transport pathway in live cells. J. Cell Biol. *147*, 743–760.

Wolf, P., and Elsässer-Beile, U. (2009). Pseudomonas exotoxin A: from virulence factor to anti-cancer agent. Int. J. Med. Microbiol. *299*, 161–176.

Yoshida, T., Chen, C.C., Zhang, M.S., and Wu, H.C. (1991). Disruption of the Golgi apparatus by brefeldin A inhibits the cytotoxicity of ricin, modeccin, and Pseudomonas toxin. Exp. Cell Res. *192*, 389–395.

Yu, S., Satoh, A., Pypaert, M., Mullen, K., Hay, J.C., and Ferro-Novick, S. (2006). mBet3p is required for homotypic COPII vesicle tethering in mammalian cells. J. Cell Biol. *174*, 359–368.

Zhang, Y., Zhu, X., Torelli, A.T., Lee, M., Dzikovski, B., Koralewski, R.M., Wang, E., Freed, J., Krebs, C., Ealick, S.E., and Lin, H. (2010). Diphthamide biosynthesis requires an organic radical generated by an iron-sulphur enzyme. Nature *465*, 891–896.

Zhao, L., and Haslam, D.B. (2005). A quantitative and highly sensitive luciferase-based assay for bacterial toxins that inhibit protein synthesis. J. Med. Microbiol. *54*, 1023–1030.